



Optimizing Photoluminescence Quantum Yields in Uranyl Dicarboxylate Complexes: Further Investigations of 2,5-, 2,6-and 3,5-Pyridinedicarboxylates and 2,3-Pyrazinedicarboxylate/fr

Pierre Thuéry, Youssef Atoini, Sotaro Kusumoto, Shinya Hayami, Yang Kim, Jack Harrowfield

► To cite this version:

Pierre Thuéry, Youssef Atoini, Sotaro Kusumoto, Shinya Hayami, Yang Kim, et al.. Optimizing Photoluminescence Quantum Yields in Uranyl Dicarboxylate Complexes: Further Investigations of 2,5-, 2,6-and 3,5-Pyridinedicarboxylates and 2,3-Pyrazinedicarboxylate/fr. European Journal of Inorganic Chemistry, 2020, 2020 (46), pp.4391-4400. cea-02958532

HAL Id: cea-02958532

<https://cea.hal.science/cea-02958532>

Submitted on 6 Oct 2020

HAL is a multi-disciplinary open access archive for the deposit and dissemination of scientific research documents, whether they are published or not. The documents may come from teaching and research institutions in France or abroad, or from public or private research centers.

L'archive ouverte pluridisciplinaire **HAL**, est destinée au dépôt et à la diffusion de documents scientifiques de niveau recherche, publiés ou non, émanant des établissements d'enseignement et de recherche français ou étrangers, des laboratoires publics ou privés.

Optimizing Photoluminescence Quantum Yields in Uranyl Dicarboxylate Complexes: Further Investigations of 2,5-, 2,6- and 3,5-Pyridinedicarboxylates and 2,3-Pyrazinedicarboxylate

Dr. Pierre Thuéry,^{*,[a]} Dr. Youssef Atoini,^[b] Sotaro Kusumoto,^[c] Pr. Dr. Shinya Hayami,^[c] Dr.

Yang Kim^[c] and Dr. Jack Harrowfield^{*,[b]}

^[a] Université Paris-Saclay, CEA, CNRS, NIMBE, 91191 Gif-sur-Yvette, France

E-mail: pierre.thuery@cea.fr, <http://iramis.cea.fr/nimbe/>

^[b] ISIS, Université de Strasbourg, 8 allée Gaspard Monge, 67083 Strasbourg, France

E-mail: harrowfield@unistra.fr, <https://isis.unistra.fr/fr/>

^[c] Department of Chemistry, Graduate School of Science and Technology, Kumamoto University, 2-

39-1 Kurokami, Chuo-ku, Kumamoto 860-8555, Japan

<http://www.sci.kumamoto-u.ac.jp/~hayami/index.html>

Keywords: Uranyl cation / Carboxylic acids / Structure elucidation / Photoluminescence

Abstract

The 2,5-, 2,6-, and 3,5-pyridinedicarboxylic (2,5-, 2,6- and 3,5-pydcH₂), and 2,3-pyrazinedicarboxylic (2,3-pyzdcH₂) acids have been used to synthesize six uranyl ion complexes including various counterions under solvo-hydrothermal conditions. While [NH₄]₂[UO₂(2,6-pydc)₂·3H₂O] (**1**) is a discrete, mononuclear species, [UO₂(2,6-pydc)₂Cu(*R,S*-Me₆cyclam))] (**2**) crystallizes as a monoperiodic coordination polymer through axial bonding of copper(II) to carboxylate donors. [PPh₃Me][UO₂(OH)(2,5-pydc)]·H₂O (**3**) and [Ni(*R,S*-Me₆cyclam)][UO₂(OH)(2,5-pydc)]₂·2H₂O (**4**) contain di-hydroxo-bridged dinuclear uranyl subunits assembled into homometallic, monoperiodic polymers. [(UO₂)₂(3,5-pydc)₂(HCOO)₂Ni(*R,S*-Me₆cyclam))] (**5**) crystallizes as a heterometallic diperiodic network with the V₂O₅ topology, and [PPh₄][UO₂(OH)(2,3-pyzdc)] (**6**) is a diperiodic species with **sql** topology. All complexes have well-resolved uranyl emission spectra in the solid state, and three of them have photoluminescence quantum yields among the highest reported for uranyl carboxylate complexes, 44% for **1**, 71% for **3**, and 36% for **6**.

Introduction

The distinctive photoluminescence properties of the uranyl ion, a cation with a characteristic green emission arising from ligand-to-metal charge transfer and plainly visible in uranyl-containing glasses, have been known for long and studied in depth in recent years.^[1] A particular feature of uranyl emission spectra is the presence of a fine structure arising from vibrational coupling, which generally results in a well-resolved pattern of at least four intense peaks. Associated with the richness of uranyl coordination chemistry, encompassing in particular a wide range of coordination polymers of varying periodicity,^[2] as well as polynuclear closed species,^[3] these luminescence properties have potential application in chemical sensors or other photoactive systems,^[4] among which species able to detect ionizing radiation^[5] or D₂O,^[6] or displaying aggregation-induced emission^[7] can be singled out. The study of the emission properties of mixed uranyl–lanthanide systems is also an active field of research.^[8] In the particular case of cavity-defining, uranyl-containing polynuclear discrete species or porous frameworks, applications as selective heterogeneous photo-oxidation catalysts^[9] could be contemplated.^[10] Indeed, several reports describe photocatalytic uses of uranyl-containing frameworks,^[11] particularly for degradation of pollutants. In this regard, uranyl complexes with high solid state photoluminescence quantum yields (PLQYs) are highly desirable, but these values are seldom reported and, when they are measured, they are often low. If the PLQY of crystalline uranyl nitrate hexahydrate (24%)^[12] is taken as a reference, only five carboxylate complexes, all polymeric, have comparable or higher PLQYs, these complexes involving the ligands (1*R*,3*S*)-(+)-camphorate (23%),^[12] 1,2,4-benzenetricarboxylate (35%),^[13] 2,6-pyridinedicarboxylate (42%),^[12] succinate (49%),^[5a] and 1,3,5-benzenetricarboxylate (58%).^[5b] It is notable however that a PLQY close to 100% has been measured for a photoluminescent borate framework in

which uranyl ions were introduced as activators.^[14] In view of the high PLQY measured^[12] for the 2,6-pyridinedicarboxylate complex $[\text{UO}_2\text{Rb}_2(2,6\text{-pydc})_2]$,^[15] it seemed worthwhile to synthesize other complexes with this ligand or its positional isomers, the interest being both to further investigate the polymeric assemblies formed by these ligands and possibly to obtain high PLQY values. We report herein the synthesis, crystal structure, emission spectrum and PLQY in the solid state of five uranyl ion complexes with the deprotonated forms of 2,6-, 2,5- and 3,5-pyridinedicarboxylic acids (2,6-, 2,5- and 3,5-pydcH₂, also known as dipicolinic, isocinchomeric, and dinicotinic acids, respectively), and of one complex with the dianion of the related 2,3-pyrazinedicarboxylic acid (2,3-pyzdcH₂). A search of the Cambridge Structural Database (CSD, version 5.41^[16]) shows that uranyl complexes of the 2,6 isomer have been the most investigated, with 46 examples reported, among which a helical monoperiodic species is particularly notable,^[17] whereas only three examples are known with the 2,5 isomer^[18] and one with the 3,5 isomer.^[8b] As for 2,3-pyrazinedicarboxylate, only three of its uranyl ion complexes have been characterized^[19] (some examples with pyrazinecarboxylate^[20] and pyrazinetetracarboxylate^[21] are also known, and the uranyl ion complexes with the derivatives 2,3-pyrazino[1,10]phenanthroline-2,3-dicarboxylate and 2,6-bis(2-pyrazinyl)pyridine-4-benzoate have been shown to be usable for nitroaromatics detection through fluorescence quenching^[22]). In order to generate complexes with structures different from those already known, different counterions were used in the present work, i.e. ammonium, phosphonium (PPh_4^+ and PPh_3Me^+), and $[\text{M}(\text{R},\text{S}-\text{Me}_6\text{cyclam})]^{2+}$ ($\text{M} = \text{Ni}, \text{Cu}$; $\text{R},\text{S}-\text{Me}_6\text{cyclam}$ (meso isomer) = 7(*R*),14(*S*)-5,5,7,12,12,14-hexamethyl-1,4,8,11-tetraazacyclotetradecane). The complexes thus obtained are zero-, mono- or diperiodic, and one of them has, to the best of our knowledge, the highest PLQY reported up to now for a uranyl ion carboxylate complex.

Results and Discussion

Syntheses

Crystals of all complexes were grown under solvo-hydrothermal conditions at a temperature of 140 °C, the crystals being formed directly from the pressurized and heated reaction mixtures and not as a result of subsequent cooling. The organic cosolvents used were either acetonitrile (**1** and **2**) or *N,N*-dimethylformamide (DMF) (**3–6**), with the occurrence in two complexes of solvent degradation products, i.e. ammonium from acetonitrile in **1**, and formate from DMF in **5**, both being usual outcomes in such reactions.^[12] Three complexes (**3**, **4** and **6**) include hydroxo anions, the ensuing oligomerization being however reduced to dimerization in all cases. Under conditions, as here, where uranyl ion is reacted with simple polycarboxylic acids without addition of base to deprotonate the acid, hydrolysis of the uranyl ion is usually prevented but here may be a consequence of the presence of the pyridine or pyrazine units. The metal/ligand stoichiometry of 7:10 in all the syntheses was chosen so as to favor the formation of an anionic uranium polycarboxylate species and consequent inclusion of counterions, which indeed occurs in all cases, although the metal/ligand stoichiometry in the final complex is either 1:2 (**1** and **2**) or 1:1 (**3–6**), the extra negative charge in the latter cases being provided by the hydroxide or formate anions. In the search for complexes with high solid state PLQY values, a useful practical criterion is the colour of the crystals (for illustrations, see references 5 and 7), since at least for values larger than 40% the green emission dominates the pale yellow due to uranyl ion absorption. In the present series, crystals of complexes **1**, **3** and **6** clearly showed this feature.

Crystal Structures

Complex **1**, $[\text{NH}_4]_2[\text{UO}_2(2,6\text{-pydc})_2]\cdot 3\text{H}_2\text{O}$, is a zero-periodic, centrosymmetric, discrete mononuclear complex in which the single uranyl cation is *O,N,O*-chelated by two 2,6-pydc²⁻ anions (Figure 1), the tridentate complexation mode being ubiquitous with this ligand.^[15,23]

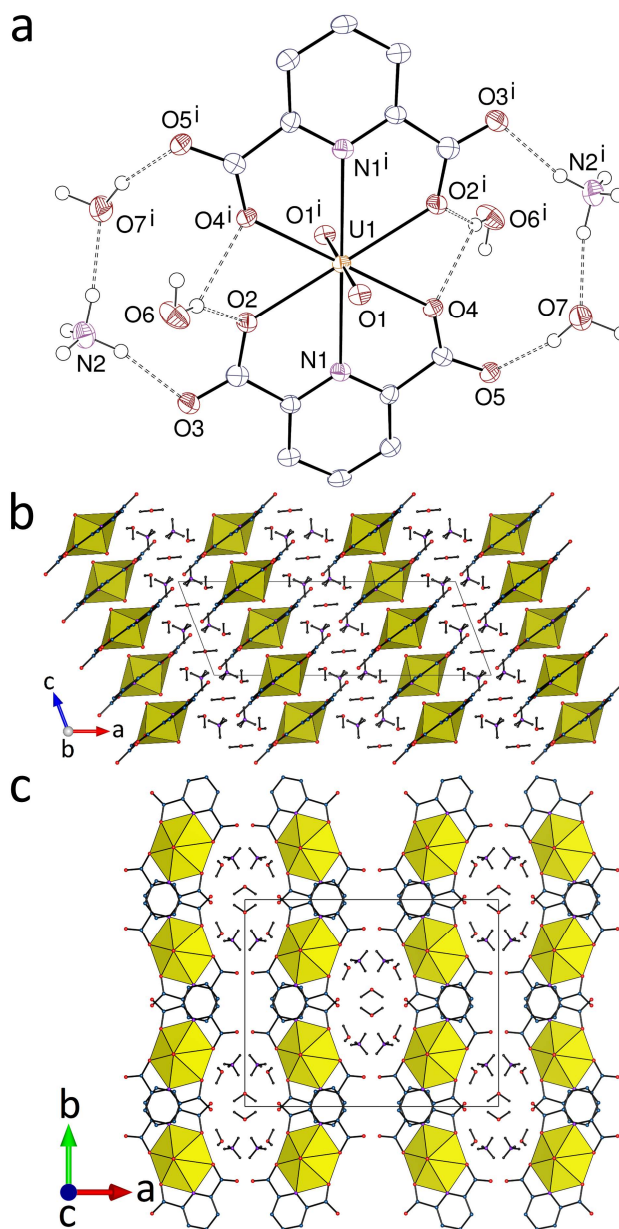


Figure 1. (a) View of complex **1**. Displacement ellipsoids are drawn at the 50% probability level. Carbon-bound hydrogen atoms are omitted and the hydrogen bonds are shown as dashed lines. Symmetry code: $i = 1/2 - x, 1/2 - y, 1 - z$. (b) and (c) Two views of the packing with uranium coordination polyhedra colored yellow.

The uranium atom is thus in a hexagonal bipyramidal coordination environment, with bond lengths in the usual range [U–O(oxo) 1.774(3) Å, U–O(carboxylato) 2.421(2) and 2.472(2) Å, U–N 2.667(3) Å]. The UO_4N_2 motif is nearly planar, with a root mean square (rms) deviation of 0.03 Å, the coordinating atoms being slightly displaced from the mean plane in chair fashion. One water molecule forms a bifurcated hydrogen bond with atoms O2 and O4ⁱ bound to uranyl, thus creating a ring with the graph set descriptor^[24] $R_1^2(4)$, and it forms another bond with the uncoordinated atom O5 of another complex unit. A second, wider ring, with the descriptor $R_3^3(12)$, results from the connection of the uncoordinated carboxylate atoms O3 and O5ⁱ by the ammonium cation and a second water molecule located on a twofold rotation axis (O7). Further hydrogen bonding of ammonium and water to carboxylate groups from different units results in the formation of a triperiodic network [O...O distances 2.757(3)–3.003(3) Å, O–H...O angles 137–166°; N...O 2.782(3)–3.219(3) Å, N–H...O 148–175°]. Calculation of short contacts with PLATON^[25] indicates the presence of parallel-displaced π -stacking interactions involving the complex anions located in the sheets parallel to (100) [centroid...centroid distance of closest pyridine rings 3.6102(16) Å, dihedral angle 5.30(14)°, slippage 1.10 Å]. Examination of the Hirshfeld surfaces (HS)^[26] calculated with CrystalExplorer (Version 3.1)^[27] shows that CH...O hydrogen bonds,^[28] generally prevalent in uranyl carboxylate complexes, are absent here. With a Kitaigorodski packing index (KPI, calculated with PLATON) of 0.74, the structure has no free space.

The same arrangement of two 2,6-pydc²⁻ ligands around uranyl is found in [$\text{UO}_2(2,6\text{-pydc})_2\text{Cu}(R,S\text{-Me}_6\text{cyclam})$] (**2**), shown in Figure 2. Here also, the uranium atom is located on an inversion centre, and the bond lengths are unremarkable [U–O(oxo) 1.775(5) Å, U–O(carboxylato) 2.462(5) and 2.468(5) Å, U–N 2.664(6) Å]. The equatorial donors are in a chair conformation and the mean UO_4N_2 plane has a rms deviation of 0.15 Å. The copper(II) cation

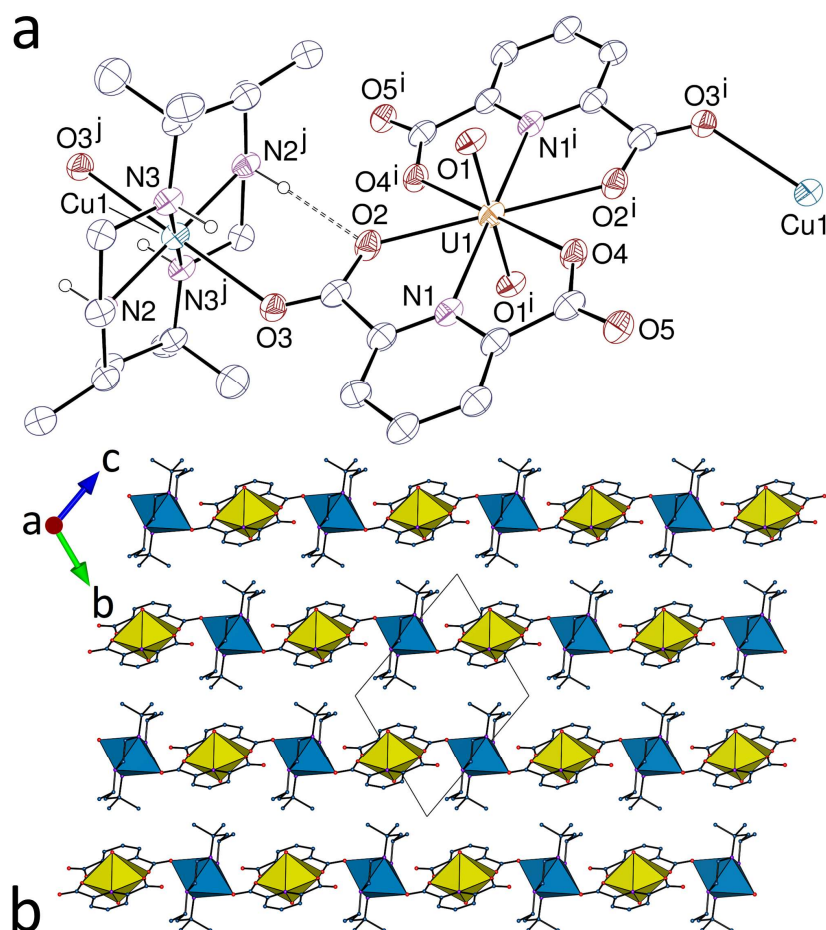


Figure 2. (a) View of complex **2**. Displacement ellipsoids are drawn at the 30% probability level. Carbon-bound hydrogen atoms are omitted and the hydrogen bond is shown as a dashed line. Symmetry codes: $i = -x, 1 - y, 2 - z$; $j = -x, -y, 1 - z$. (b) View of the packing of the heterometallic chains with uranium coordination polyhedra yellow and those of copper blue.

is bound to the four nitrogen atoms of the macrocycle and makes two longer axial contacts with two carboxylate oxygen atoms, its environment being axially elongated octahedral [Cu–N 2.044(6) and 2.056(6) Å, Cu–O 2.451(5) Å]. Each $\text{UO}_2(2,6\text{-pydc})_2^{2-}$ fragment is thus linked to two copper(II) cations, through two carboxylate groups bound in syn/anti $\mu_2\text{-}\kappa^1\text{O}:\kappa^1\text{O}'$ mode, resulting in the formation of a monoperiodic coordination polymer parallel to [011]. This arrangement is reminiscent of that found in other uranyl complexes with $2,6\text{-pydc}^{2-}$ incorporating 3d-block metal cations.^[23b,23g] As usual when a metal azamacrocycle complex

is bound to a uranyl-containing motif, hydrogen bonds may contribute to the stability of the assembly, in particular that involving atoms N2^j and O2 [N...O 2.969(8) Å, N–H...O 177°]. The chains are arranged in sheets parallel to (01 $\bar{1}$), within which chains adjacent along [100] are involved in parallel-displaced π -stacking interactions [centroid...centroid distance 3.468(5) Å, dihedral angle 0°, slippage 1.22 Å], and the packing is compact (KPI 0.69).

The complexes **1** and **2** are additions to a quite large family^[15,23] of species containing the mononuclear [UO₂(2,6-pydc)₂]²⁻ anion. Given the many similarities between NH₄⁺ and K⁺ as structural entities, the structure of complex **1** could be regarded as completing structural characterization of the sub-group of this family involving the alkali metals as counter cations.^[15,23d,23e] Crystals of complex **1** certainly have the same greenish-yellow colour as have those of its K⁺ analogue, though this is a colour which, visually, is the same for the whole alkali metal family (as well as H⁺),^[15] and is shared by the related materials involving [AsPh₄]⁺ and [HNEt₃]⁺ countercations,^[23a,29] though not that involving acridinium,^[23c] where the colour appears to be dominated by that of the cation. These species do not form an isomorphous series but a striking feature of all the structures is the presence of extended stacking arrays of the [UO₂(2,6-pydc)₂]²⁻ units, which are close to planar in all except for [HNEt₃]₂[UO₂(2,6-pydc)₂], where they are appreciably bowed. Another feature is that the shortest U...U separation is ~7 Å or greater, on the high side for most uranyl carboxylate complexes and considerably exceeding that in [UO₂(NO₃)₂(H₂O)₂].4H₂O (6.092 Å),^[30] for example. The possible significance of both these features in relation to PLQY values is discussed ahead.

Uranyl *O,N,O*-chelation is no longer possible with the 2,5-pydc²⁻ isomer in [PPh₃Me][UO₂(OH)(2,5-pydc)]·H₂O (**3**), and the unique uranyl cation is here *O,N*-chelated by the nitrogen atom and the adjacent carboxylate group, and bound to one oxygen atom of

the carboxylate in the 5 position of another ligand, and to two hydroxide anions [U–O(oxo) 1.7860(17) and 1.7878(17) Å, U–O(carboxylato) 2.3779(18) and 2.3984(17) Å, U–O(hydroxo) 2.2868(17) and 2.3147(17), U–N 2.601(2) Å], its environment being thus pentagonal bipyramidal (Figure 3). Such dinuclear uranyl subunits with double hydroxo bridges are very

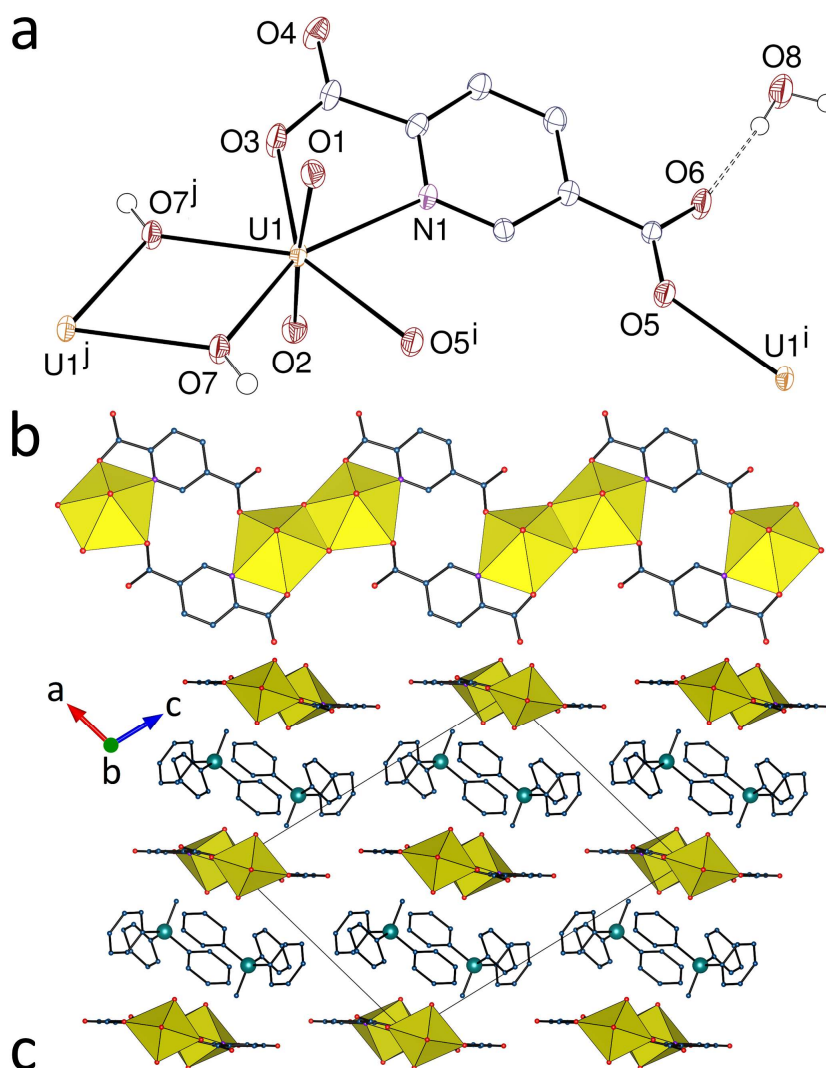


Figure 3. (a) View of complex **3** with counterions omitted. Displacement ellipsoids are drawn at the 50% probability level. Carbon-bound hydrogen atoms are omitted and the hydrogen bond is shown as a dashed line. Symmetry codes: $i = 1 - x, 1 - y, 1 - z$; $j = 1 - x, -y, 1 - z$. (b) View of the monoperic coordination polymer. (c) Packing with chains viewed end-on. Uranium coordination polyhedra are yellow and phosphorus atoms are blue.

common,^[2c] and some examples have been found with the 2,6-pydc²⁻ isomer.^[29] Here again, a monoperiodic coordination polymer is formed, which runs along [010] and has the shape of a quasi-planar ribbon containing a succession of 12-membered rings. These chains are arranged into sheets parallel to (101), separated from one another by layers of counterions (KPI 0.70). The hydroxide anion is hydrogen bonded to the O6 atom of a ligand bound to the same uranyl cation ($R_1^1(6)$ ring), and the water molecule bridges atom O6 and atoms O3 and O4 in the same chain [O...O 2.685(2)–3.102(3) Å, O–H...O 145(4)–166(4)°]. The 2,5-pydc²⁻ ligand is not involved in any π -stacking interaction, but the PPh₃Me⁺ cations are arranged in zigzag rows parallel to [010], with a P...P distance of 7.4380(8) Å, held by parallel-displaced π -stacking interactions [centroid...centroid 4.1566(15) Å, dihedral angle 23.18(12)°], an arrangement similar to the “phenyl embraces” found with PPh₄⁺.^[31] The HS shows the presence of several CH...O hydrogen bonds, in particular one involving the methyl group of the cation and the uranyl oxo atom O1 [C...O 3.460(3) Å, C–H...O 169°].

The complex [Ni(*R,S*-Me₆cyclam)][UO₂(OH)(2,5-pydc)]₂·2H₂O (**4**) displays structural features close to those of **3**. The unique uranyl cation is similarly *O,N*-chelated by one ligand and bound to another carboxylate donor and two hydroxide anions [U–O(oxo) 1.749(7) and 1.770(7) Å, U–O(carboxylato) 2.408(7) and 2.408(6) Å, U–O(hydroxo) 2.288(6) and 2.330(7), U–N 2.632(8) Å] (Figure 4). A ribbon-like, monoperiodic coordination polymer running along [100] is formed, which displays a shape slightly different to that in **3**. In the latter complex, the two bridging ligands in a ring are bound to only one uranyl cation from each dinuclear subunit, these subunits being only slightly inclined with respect to the chain axis, while in **4** they are perpendicular to it and each bridging ligand is bound to a different uranyl cation in the dimer, thus forming larger, 16-membered rings. While the uncoordinated atom O6 of

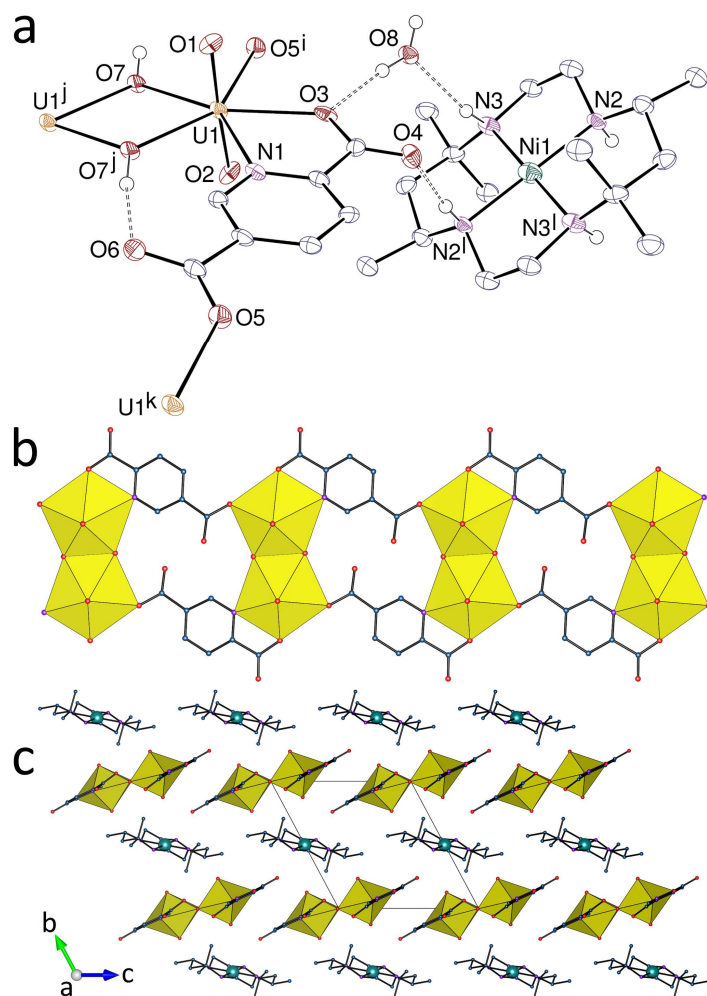


Figure 4. (a) View of complex **4**. Displacement ellipsoids are drawn at the 50% probability level. Carbon-bound hydrogen atoms are omitted and hydrogen bonds are shown as dashed lines. Symmetry codes: $i = x - 1, y, z$; $j = -x, -y, -z$; $k = x + 1, y, z$; $l = 1 - x, 1 - y, 2 - z$. (b) View of the monoperiodic coordination polymer. (c) Packing with chains viewed end-on. Uranium coordination polyhedra are yellow and nickel atoms are shown as blue spheres.

the non-chelating, monodentate carboxylate group is directed outward from the 12-membered ring in **3**, it is oriented inside the ring in **4** and hydrogen bonded to the hydroxide anion [$O7^j \cdots O6$ 2.685(9) Å, $O7^j-H \cdots O6$ 148(12)°; $R_1^1(8)$ ring]. In contrast to copper(II) in **2**, nickel(II), located on an inversion centre, is only bound to the four nitrogen atoms of the macrocycle [Ni–N 1.959(8) and 1.990(9) Å], so that bridging of the chains is achieved through

hydrogen bonding only, either directly or via a water molecule [$N\cdots O$ 2.863(12) and 2.909(11) Å, $N-H\cdots O$ 161(11) and 173(11)°], with formation of $R_3^3(10)$ rings. The packing (KPI 0.74) displays an alternation of anionic and cationic sheets parallel to (010). With a centroid \cdots centroid distance of 4.550(6) Å and a large slippage of 3.12 Å, the possible intra-sheet π -stacking interaction may not be significant.

N,O-Chelation is precluded with the 3,5 isomer of the ligand, and the unique uranyl cation in $[(UO_2)_2(3,5\text{-pydc})_2(HCOO)_2Ni(R,S\text{-Me}_6\text{cyclam})]$ (**5**) is chelated by one carboxylate group and bound to two oxygen donors from two more 3,5-pydc²⁻ ligands, and to one from a formate anion, its environment being pentagonal bipyramidal [$U-O(\text{oxo})$ 1.7653(18) and 1.7737(18) Å, $U-O(\text{carboxylato})$ 2.4426(16) and 2.4887(17) Å for the chelating group, 2.3190(18)–2.3455(16) Å for the other groups] (Figure 5). Uranyl and 3,5-pydc²⁻ ligands

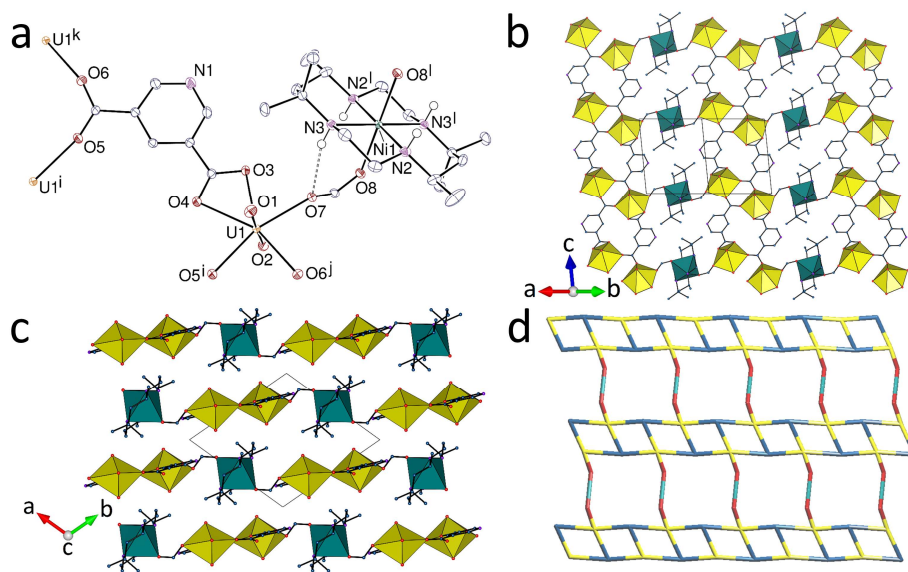


Figure 5. (a) View of complex **5**. Displacement ellipsoids are drawn at the 50% probability level. Carbon-bound hydrogen atoms are omitted and the hydrogen bond is shown as a dashed line. Symmetry codes: $i = 2 - x, 1 - y, 1 - z$; $j = x, y, z + 1$; $k = x, y, z - 1$; $l = 1 - x, 2 - y, 2 - z$. (b) View of the diperiodic assembly with uranium coordination polyhedra in yellow and those of nickel in green. (c) Packing with layers viewed edge-on. (d) Nodal representation of the network (yellow, uranium nodes; dark blue, dicarboxylate nodes; green, nickel links, red, formate links).

alone form ribbon-like chains parallel to [001] with double bridging of the cations resulting in an alternation of centrosymmetric 8- and 16-membered rings, analogous to that found in the other known complex with this ligand.^[8b] The nickel(II) cation, located on an inversion centre, is in a slightly elongated octahedral environment, with four basal nitrogen donors and two axial formate donors [Ni–N 2.061(2) and 2.085(2) Å, Ni–O 2.1690(17) Å]. The formate bridge between uranium and nickel has a syn(Ni)/anti(U) conformation similar to that seen in other heterometallic complexes,^[12] or in simple uranyl formate species.^[32] Ni^{II} cations thus bridge the uranyl-containing chains to form a diperiodic 3,4-coordinated network parallel to (110), which has the point symbol {4².6³.8}{4².6} and the V₂O₅ topology. This topological type is frequently encountered when monoperiodic uranyl-containing chains are linked by additional cations.^[13,33] One of the NH groups of the macrocycle is hydrogen bonded to the formate oxygen atom bound to uranium (*R*₁¹(6) ring), and the other makes a bifurcated hydrogen bond with the formate oxygen atom bound to Ni^{II} and a uranyl oxo group [N...O 2.853(3)–3.098(3) Å, N–H...O 110(2)–164(3)°]. The packing is of the bump-to-hollow type, the layers being offset with respect to one another (KPI 0.70), with a possible inter-sheet π -stacking interaction [centroid...centroid 4.4647(19) Å, dihedral angle 0°, slippage 2.51 Å]. The structures of complexes **4** and **5** provide further examples of the different ways in which a given tetra-azamacrocyclic complex may contribute to a crystal array.^[34]

Although the 2,3-pyzdc²⁻ ligand could be twice *O,N*-chelated and also *O,O*-chelated by the two carboxylate groups, modes of coordination indeed observed in previously reported uranyl ion complexes,^[19] it has the same connectivity in [PPh₄][UO₂(OH)(2,3-pyzdc)] (**6**) as 2,5-pydc²⁻ in **3** and **4**. The unique uranyl cation is *O,N*-chelated by one ligand (a

coordination mode also found with the related 2,3-pydc²⁻ ligand, which is nevertheless also *O,O*-chelating^[23b]), and bound to one carboxylate oxygen atom from a second ligand and two hydroxide anions [U–O(oxo) 1.754(5) and 1.777(4) Å, U–O(carboxylato) 2.342(4) and 2.370(4) Å, U–O(hydroxo) 2.312(4) and 2.314(4), U–N 2.643(4) Å] (Figure 6). However,

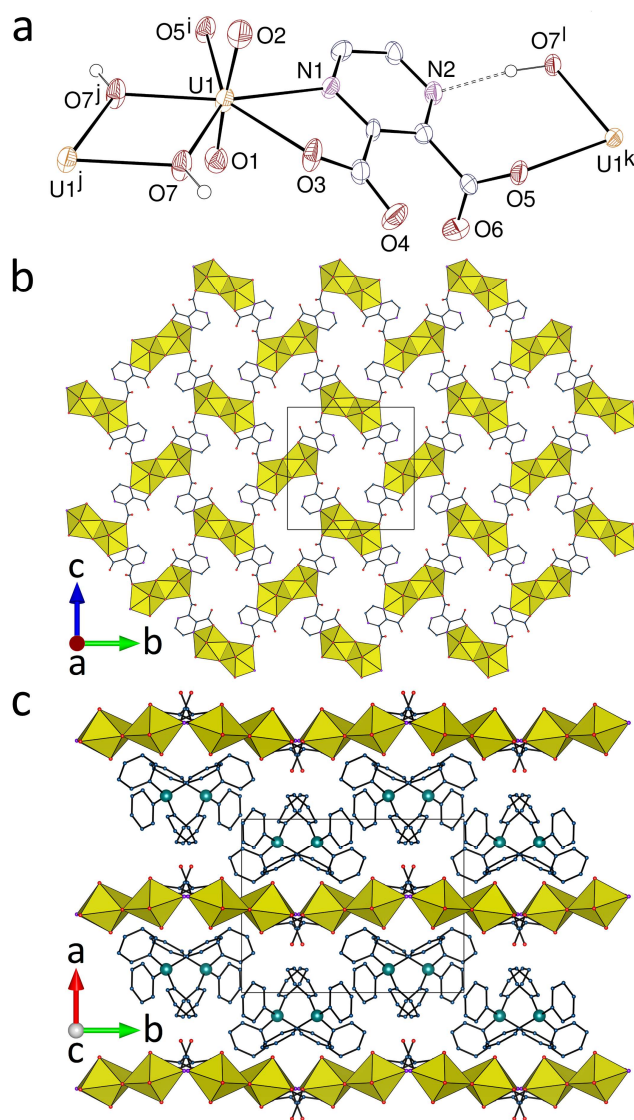


Figure 6. (a) View of complex **6**. Displacement ellipsoids are drawn at the 40% probability level. Counterions and carbon-bound hydrogen atoms are omitted, and the hydrogen bond is shown as a dashed line. Symmetry codes: $i = x, 1/2 - y, z - 1/2$; $j = 1 - x, 1 - y, -z$; $k = x, 1/2 - y, z + 1/2$; $l = 1 - x, y - 1/2, 1/2 - z$. (b) View of the diperiodic assembly. (c) View of the packing with layers edge-on. Uranium coordination polyhedra are yellow and phosphorus atoms are blue.

instead of crystallizing as a monoperiodic coordination polymer, it yields a diperiodic assembly parallel to (100) which, if the binuclear subunits are considered as single 4-coordinated nodes, has the square lattice (**sql**) topology (however, this description ignores the herringbone arrangement of the dinuclear subunits). A diperiodic network was also found with the related 2,3-pydc²⁻ ligand, but in this case no hydroxide anion is present and all carboxylate oxygen atoms are coordinated.^[23b] The uncoordinated nitrogen atom in **6** is involved in a hydrogen bond with the hydroxide anion [O...N 2.816(6) Å, O-H...N 172°; $R_1^1(7)$ ring]. The packing (KPI 0.67) shows quasi-planar sheets separated by layers of counterions, the latter being associated in twos by “phenyl embrace” interactions, with a P...P separation of 6.460(3) Å. A parallel-displaced π -stacking interaction associates the pyrazine ring and one ring of the counterion [centroid...centroid 3.940(4) Å, dihedral angle 23.9(3)°], and several CH...O hydrogen bonds also link the anions and cations.

Luminescence Properties

Emission spectra of complexes **1–6** in the solid state at room temperature under excitation at 420 nm were recorded and are shown in Figure 7. All display the commonly observed fine structure associated with the vibronic progression corresponding to the $S_{11} \rightarrow S_{00}$ and $S_{10} \rightarrow S_{0\nu}$ ($\nu = 0-4$) electronic transitions.^[1b] The most blue-shifted spectrum is that of complex **6**, with the four main maxima (corresponding to the electronic transitions denoted E and S1–S3^[1h]) at 482, 502, 524 and 547 nm, these values being more typical of a complex with an O₆ rather than an O₄N equatorial environment.^[35] The maxima in the spectrum of complex **1** are at 488, 510, 533 and 557 nm, these values being at the upper end of the range previously found for complexes with uranyl O₄N₂ equatorial environments,^[35] and similar to those

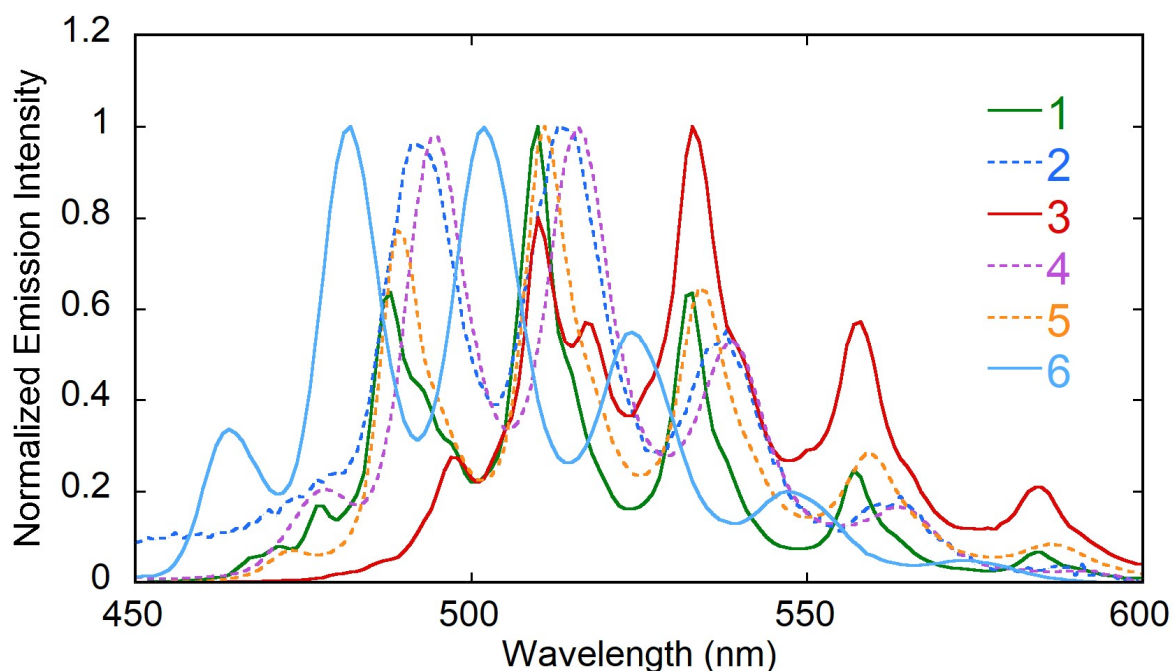


Figure 7. Normalized emission spectra of compounds **1**–**6** under excitation at 420 nm.

measured for $[\text{UO}_2(2,6\text{-pydc})]^{[23b]}$ and $[\text{UO}_2(2,6\text{-pydcH})_2]\cdot 4\text{H}_2\text{O}^{[15]}$. The most red-shifted spectrum is found for complex **3** (O_4N environment) with maxima at 510, 533, 558 and 584 nm, these values being among the most red-shifted measured for a five-coordinated uranyl cation, those for complexes with O_5 environments being generally below about 500, 520, 545 and 575 nm.^[35] The spectra of the other complexes are more slightly red-shifted with respect to that of **1**, with values of 492, 513, 538 and 561 nm for **2** (O_4N_2), 495, 516, 539 and 563 nm for **4** (O_4N), and 489, 511, 534 and 559 nm for **5** (O_5). The values for **5** in particular are typical of those generally found for complexes with O_5 environments.^[35] It is notable that the spectra of **1** and **3** are peculiar in this series since all peaks display shoulders on the low-energy side, one of these shoulders being even partly resolved for **3** (517 nm). Such shoulders, albeit less prominent, were also present in the spectra of two other uranyl complexes with the 2,6 isomer, either partly or fully deprotonated.^[15,23b] This may be significant in the light of the measurements of PLQYs, although such additional complexity in

the vibronic progression has been detected in a variety of species^[1e,1f,36] and has been attributed to coupling of the electronic transition to vibrational modes involving either the equatorial ligands bound to the uranyl centre or bending of the UO_2 unit^[1f,36] or indeed to the superposition of another vibronic progression associated with a metal-to-ligand charge transfer transition.^[23b]

While complexes **2**, **4** and **5** have low PLQYs of 4, 1 and 1%, respectively, complexes **1**, **3** and **6** have values of 44, 71 and 36%, respectively, the value for **3** being the highest yet reported for a uranyl ion carboxylate complex. The fact that the PLQY is low in **2** and **4**, which have environments similar to **1** and **3**, respectively, is likely due to the presence of 3d-block metal cations, the latter either preferentially absorbing the 420 nm radiation, or allowing energy transfer and nonradiative relaxation, often resulting in complete quenching of uranyl luminescence.^[37] Such quenching also appears to occur in complexes where $[\text{UO}_2(2,6\text{-pydc})_2]^{2-}$ units are linked by Fe^{II} , Co^{II} , Ni^{II} , Cu^{II} or Zn^{II} bridges,^[23g] since the colours of the isolated crystals under normal sunlight reflect those of the different transition metals and are not dominated by green emission. Complexes **1**, **3** and **6**, with organic counterions, do not suffer from this drawback.

Like all aromatic species, pyridine- and pyrazinedicarboxylate ligands may enhance uranyl luminescence through the “antenna” effect,^[1e] arising from energy transfer from excited π electrons of the ligand to the metal,^[23b] and given its apparently long-distance operation in uranyl oxyfluorides containing pyridinium as counterion,^[38] and efficacy in a uranyl complex with 2,2'-bipyrimidine,^[39] it could be possible that heteroaromatic units are more efficient in energy transfer than simple aromatic ones, though no visually obvious effects are seen with complexes of the common ligands 2,2'-bipyridine and 1,10-phenanthroline.^[40] In considering the luminescence of uranyl ion coordination polymers and

organic frameworks, it is important to note that such materials are usually insoluble in all solvents other than those which cause their decomposition, so that only solid state PLQY values can be obtained. It has been long known^[1e,41] that for simple, water-soluble uranyl complexes PLQY values in water are usually much less than those of the solid solutes and in fact we have previously observed^[15] that emission from water-soluble, mononuclear $[\text{UO}_2(2,6\text{-pydc})_2]^{2-}$ derivatives involving alkali metal cations, is much weaker in solution than in the solid. More recently,^[42] it has been shown that emission from uranyl ion complexes with $2,6\text{-pydc}^{2-}$ in acetonitrile is an order of magnitude more intense than in water. Hence, it is plausible that the high, solid state PLQY values observed for simple $[\text{UO}_2(2,6\text{-pydc})_2]^{2-}$ derivatives (presently extended to the species with countercations Li^+ , Na^+ , K^+ and Cs^+ with values of 26, 33, 27 and 38%, respectively, as well as the 44% found for complex **1**) may be a form of “aggregation enhanced luminescence” where the effect of the aggregation required to form a crystal is simply that of minimizing contact with solvent molecule quenchers (water, in particular). This is in conflict with our earlier suggestion^[15] that the extensive stacking arrays of aromatic units observed in the structures of these materials might signify interactions giving rise to an especially efficient means of energy transfer from the “antenna” to the metal ion but it is consistent with numerous more recent structure determinations showing extensive stacking arrays in complexes which are not strongly luminescent.^[43] Nonetheless, for a uranyl carboxylate complex which undergoes a single-crystal to single-crystal transformation when exposed to water,^[7] it is the hydrated product which has the higher PLQY and there are many instances in general where coordinated water has a negligible effect on emission intensity,^[1e] not to mention the moderate solid state PLQY retained in $[\text{UO}_2(\text{NO}_3)_2(\text{H}_2\text{O})_2] \cdot 4\text{H}_2\text{O}$, so that the “lack of quenchers” argument to explain the high PLQY values of variously hydrated crystalline $(\text{Cation})_2[\text{UO}_2(2,6\text{-pydc})_2]$

species must remain tentative, even though it is true that there are no direct interactions between the water molecules and uranyl oxygen atoms in any of the structures.^[15,23d,23e] In regard to interactions within the stacks of aromatic units, examination of the Hirshfeld surfaces does not provide evidence of interactions beyond dispersion, indicating that they are not unusually strong and where, in different complexes, there do appear to be additional, specific interactions, these lead not to enhancement of uranyl emission but to its replacement by emission with the characteristics of an organic fluorophore.^[44]

Emission from hydroxo/oxo-bridged oligomers of uranyl ion can have an unusual form taken to be indicative of direct electronic interactions between close uranyl centres,^[45] and an alternative explanation of the strong emission from (Cation)₂[UO₂(2,6-pydc)₂] species initially considered was that the relatively long U...U separations (~7 Å) found in the crystal structures might signify an absence of perturbations shortening excited state lifetimes due to U...U interactions. There is a rough correlation between the minimum U...U distances and the PLQY values, with the PLQY generally increasing with increasing separation but this is clearly not an argument which could be extended to explain the high PLQY values in complexes **3** (71%), [UO₂(1,3,5-btcH)] (58%, btc = benzenetricarboxylate)^[5b], [NMe₄]₂[(UO₂)₄(C₂O₄)₄(succinate)] (49%)^[5a], **6** (36 %) or [PPh₄][UO₂(1,2,4-btc)] (35%),^[13] where the minimum U...U separations are 3.85, 5.23, 5.55, 3.85 and 5.12 Å, respectively. These five complexes have features which clearly distinguish them from the (Cation)₂[UO₂(2,6-pydc)₂] family. They are all true coordination polymers of low solubility and all contain pentagonal-bipyramidal, not hexagonal-bipyramidal, U^{VI} centres. Three of the five, **3**, [UO₂(1,3,5-btcH)] and [PPh₄][UO₂(1,2,4-btc)], have structures incorporating monoperiodic polymer chains in which dinuclear units have hydroxide or carboxylate bridges, while that of [NMe₄]₂[(UO₂)₄(C₂O₄)₄(succinate)] contains monoperiodic chains of

oxalate-bridged uranium centres lying in sheets linked into a triperiodic array by succinate ligand bridging, and that of complex **6** involves diperiodic sheets where dihydroxy-bridged dinuclear units are linked by the ligands. All show a well-resolved vibronic progression in their green emissions, with little evidence (see above) that the proximity of uranium centres has any marked influence on the form of the emission bands. While there are similarities in the four monoperiodic chains, related complexes such as $[\text{PPh}_4]_2[(\text{UO}_2)_2(1,2,4\text{-btch})_3]\cdot\text{H}_2\text{O}$ ^[13] containing monoperiodic chains seemingly only slightly different, although in this instance containing hexagonal-bipyramidal uranium centres, are only weakly luminescent, so that exactly what features of the chain structures may be most important is uncertain.

Conclusions

The synthesis, crystal structure, emission spectrum, and PLQY of six uranyl ion complexes with the ligands 2,5-, 2,6- and 3,5-pyridinedicarboxylate and 2,3-pyrazinedicarboxylate have both expected and unexpected features. Solvothermal syntheses using the acids and not their conjugate bases as reactants have provided, as commonly observed with carboxylic acids, carboxylate complexes of uranyl ion but in three cases in association with a degree of hydrolysis of the cation which may reflect the influence of aza-aromatic-N. Given the high PLQY values found here for complexes containing $\text{U}(\text{OH})_2\text{U}$ units, this may be a particularly important property of these ligands. All the ligands employed except 3,5-pydc²⁻ act as chelates towards the uranyl cation in the *O,N* or *O,N,O* mode depending on whether the nitrogen atom is flanked by one or two carboxylate groups but in the pyrazinedicarboxylate one nitrogen atom remains uncoordinated, consistent with the oxophilic character of uranyl ion. Except for complex **1** which is a discrete anionic mononuclear species, all the complexes are anionic coordination polymers, with periodicities of 1 (**2**, **3** and **4**) or 2 (**5** and **6**) and low

solubility, rendering them of potential interest as heterogeneous photo-oxidation catalysts. Various counteranions are included, which play different roles in the structures: NH_4^+ in **1** and $\text{Ni}(R,S\text{-Me}_6\text{cyclam})^{2+}$ in **4** interact with the anion through hydrogen bonding, PPh_3Me^+ in **3** and PPh_4^+ in **6** are organized in sheets loosely interacting with the anionic layers through $\text{CH}\cdots\text{O}$ hydrogen bonds and π -stacking interactions, and $\text{Cu}(R,S\text{-Me}_6\text{cyclam})^{2+}$ in **2** and $\text{Ni}(R,S\text{-Me}_6\text{cyclam})^{2+}$ in **5** are part of the coordination polymers. All six complexes have well-resolved uranyl emission spectra in the solid state, but the PLQYs are widely different. While complexes **2**, **4** and **5** have low PLQY values of 4, 1 and 1%, respectively, probably because of the presence of 3d-block transition metal cations in the structure, complexes **1**, **3** and **6**, with organic counterions, have values of 44, 71 and 36%, respectively, that for **3** being the highest reported for a uranyl ion carboxylate complex. Consideration of the structures of **1**, **3** and **6** along with those of other known species having high PLQY values is hampered by the limited extent of current data but complexes of 2,6-pydc²⁻ containing hexagonal-bipyramidal U^{VI} appear to emit strongly when in a structure where they are well separated (and where transition metal ions are not present) while, somewhat paradoxically, complexes of other aza-aromatic dicarboxylates containing pentagonal-bipyramidal U^{VI} emit strongly (in the presence of organic counter cations) when binuclear species bridged by hydroxide or carboxylate are present.

Experimental Section

General: $\text{UO}_2(\text{NO}_3)_2 \cdot 6\text{H}_2\text{O}$ (RP Normapur, 99%) was purchased from Prolabo, and the dicarboxylic acids were from Merck or Aldrich. $[\text{M}(R,S\text{-Me}_6\text{cyclam})(\text{NO}_3)_2]$ ($\text{M} = \text{Ni}, \text{Cu}$) were synthesized as previously described.^[33b,46] Elemental analyses were performed by MEDAC Ltd. at Chobham, UK. For all syntheses, the mixtures in demineralized water were placed in

10 mL tightly closed glass vessels and heated at 140 °C in a sand bath, under autogenous pressure.

Caution! Uranium is a radioactive and chemically toxic element, and uranium-containing samples must be handled with suitable care and protection.

[NH₄]₂[UO₂(2,6-pydc)₂]₂·3H₂O (1): 2,6-pydcH₂ (17 mg, 0.10 mmol), UO₂(NO₃)₂·6H₂O (35 mg, 0.07 mmol), and PPh₄Br (42 mg, 0.10 mmol) were dissolved in a mixture of water (0.8 mL) and acetonitrile (0.2 mL), giving green-yellow crystals of complex **1** within one month (13 mg, 38% yield based on the acid). C₁₄H₂₀N₄O₁₃U (690.37): calcd. C 24.36, H 2.92, N 8.12; found C 24.01, H 2.70, N 7.93.

[UO₂(2,6-pydc)₂Cu(*R,S*-Me₆cyclam)] (2): 2,6-pydcH₂ (17 mg, 0.10 mmol), UO₂(NO₃)₂·6H₂O (35 mg, 0.07 mmol), and [Cu(*R,S*-Me₆cyclam)(NO₃)₂] (24 mg, 0.05 mmol) were dissolved in a mixture of water (0.8 mL) and acetonitrile (0.2 mL), giving light purple crystals of complex **2** in low yield within two weeks.

[PPh₃Me][UO₂(OH)(2,5-pydc)]·H₂O (3): 2,5-pydcH₂ (17 mg, 0.10 mmol), UO₂(NO₃)₂·6H₂O (35 mg, 0.07 mmol), and PPh₃MeBr (36 mg, 0.10 mmol) were dissolved in a mixture of water (0.8 mL) and DMF (0.2 mL), giving green-yellow crystals of complex **3** within ten days (22 mg, 42% yield based on U). Elemental analysis results indicate the presence of a small amount of water in excess of the quantity found from crystal structure determination. C₂₆H₂₄NO₈PU + 0.5H₂O (756.46): calcd. C 41.28, H 3.33, N 1.85; found C 41.18, H 3.15, N 1.57.

[Ni(*R,S*-Me₆cyclam))][UO₂(OH)(2,5-pydc)]₂·2H₂O (4): 2,5-pydcH₂ (17 mg, 0.10 mmol), UO₂(NO₃)₂·6H₂O (35 mg, 0.07 mmol), and [Ni(*R,S*-Me₆cyclam)(NO₃)₂] (23 mg, 0.05 mmol) were dissolved in a mixture of water (0.8 mL) and DMF (0.2 mL), giving orange crystals of complex **4** overnight (24 mg, 53% yield based on U). C₃₀H₄₈N₆NiO₁₆U₂ (1283.51): calcd. C 28.07, H 3.77, N 6.55; found C 27.75, H 3.71, N 6.26.

[(UO₂)₂(3,5-pydc)₂(HCOO)₂Ni(*R,S*-Me₆cyclam))] (**5**): 3,5-pydcH₂ (17 mg, 0.10 mmol), UO₂(NO₃)₂·6H₂O (35 mg, 0.07 mmol), and [Ni(*R,S*-Me₆cyclam)(NO₃)₂] (23 mg, 0.05 mmol) were dissolved in a mixture of water (0.8 mL) and DMF (0.2 mL), giving yellow crystals of complex **5** within two months (21 mg, 46% yield based on U). C₃₂H₄₄N₆NiO₁₆U₂ (1303.50): calcd. C 29.49, H 3.40, N 6.45; found C 28.82, H 3.33, N 5.84.

[PPh₄][UO₂(OH)(2,3-pydc)] (**6**): 2,3-pydcH₂ (17 mg, 0.10 mmol), UO₂(NO₃)₂·6H₂O (35 mg, 0.07 mmol), and PPh₄Br (42 mg, 0.10 mmol) were dissolved in a mixture of water (0.8 mL) and DMF (0.2 mL), giving yellow-green crystals of complex **6** in low yield within one month.

Crystallography: The data were collected at 100(2) K, either on a Nonius Kappa-CCD area detector diffractometer^[47] using graphite-monochromated Mo K α radiation (λ = 0.71073 Å) (complexes **1**, **2** and **6**) or on a Bruker D8 Quest diffractometer equipped with an Incoatec Microfocus Source (I μ S 3.0 Mo) and a PHOTON III area detector, and operated through the APEX3 software^[48] (complexes **3–5**). The crystals were mounted into glass capillaries or on Mitegen micromounts with a protective coating of Paratone-N oil (Hampton Research). The data were processed with HKL2000^[49] or SAINT,^[50] and absorption effects were corrected for empirically with SCALEPACK^[49] or SADABS.^[51] The structures were solved by intrinsic phasing

with SHELXT,^[52] expanded by subsequent difference Fourier synthesis and refined by full-matrix least-squares on F^2 with SHELXL,^[53] using the ShelXle interface.^[54] All non-hydrogen atoms were refined with anisotropic displacement parameters. When present, the hydrogen atoms bound to oxygen and nitrogen atoms were found on difference Fourier maps and they were either refined isotropically (with restraints if necessary) or treated as riding atoms. The carbon-bound hydrogen atoms were introduced at calculated positions and were treated as riding atoms with an isotropic displacement parameter equal to 1.2 times that of the parent atom (1.5 for CH₃, with optimized geometry). Crystal data and structure refinement parameters are given in Table 1. The molecular plots were drawn with ORTEP-3^[55] and the polyhedral representations with VESTA.^[56] Topological analyses were conducted with ToposPro.^[57]

Table 1. Crystal data and structure refinement details.

	1	2	3	4	5	6
Empirical formula	C ₁₄ H ₂₀ N ₄ O ₁₃ U	C ₃₀ H ₄₂ CuN ₆ O ₁₀ U	C ₂₆ H ₂₄ NO ₈ PU	C ₃₀ H ₄₈ N ₆ NiO ₁₆ U ₂	C ₃₂ H ₄₄ N ₆ NiO ₁₆ U ₂	C ₃₀ H ₂₃ N ₂ O ₇ PU
M (g mol ⁻¹)	690.37	948.26	747.46	1283.51	1303.50	792.50
Crystal system	monoclinic	triclinic	monoclinic	triclinic	triclinic	monoclinic
Space group	$C2/c$	$P\bar{1}$	$P2_1/n$	$P\bar{1}$	$P\bar{1}$	$P2_1/c$
a (Å)	19.7887(10)	8.8164(7)	13.3789(5)	9.4943(9)	9.8450(4)	12.4003(6)
b (Å)	15.0804(9)	9.6895(7)	11.1183(3)	10.7752(10)	10.7454(4)	15.3937(5)
c (Å)	7.2190(3)	10.8668(9)	17.7408(6)	11.3208(11)	11.1116(5)	15.2945(7)
α (°)	90	106.756(5)	90	112.140(4)	113.8760(14)	90
β (°)	110.736(4)	100.254(5)	104.5117(13)	113.689(4)	103.4168(15)	103.414(3)
γ (°)	90	100.894(6)	90	97.248(4)	101.8885(15)	90
V (Å ³)	2014.75(19)	845.77(12)	2554.76(15)	928.27(16)	984.32(7)	2839.9(2)
Z	4	1	4	1	1	4
Reflections collected	32991	34596	149960	48374	99401	54909
Independent reflections	1918	3211	6592	3507	6015	5384
Observed reflections [$I > 2\sigma(I)$]	1507	2745	5679	3168	5587	4250
R_{int}	0.057	0.062	0.070	0.100	0.048	0.060
Parameters refined	147	223	347	268	270	370
R_1	0.021	0.048	0.019	0.046	0.017	0.037
wR_2	0.050	0.115	0.036	0.115	0.037	0.084
S	0.978	1.006	1.074	1.136	1.189	1.042
$\Delta\rho_{min}$ (e Å ⁻³)	-1.21	-2.79	-0.79	-2.42	-1.39	-2.19
$\Delta\rho_{max}$ (e Å ⁻³)	0.71	1.74	1.51	3.66	2.21	1.36

CCDC 2024614 (for **1**), 2024615 (for **2**), 2024616 (for **3**), 2024617 (for **4**), 2024618 (for **5**), and 2024619 (for **6**) contain the supplementary crystallographic data for this paper. These

data can be obtained free of charge from The Cambridge Crystallographic Data Centre via www.ccdc.cam.ac.uk/data_request/cif.

Luminescence Measurements: Emission spectra were recorded on solid samples using a Horiba-Jobin-Yvon IBH FL-322 Fluorolog 3 spectrometer equipped with a 450 W xenon arc lamp, double-grating excitation and emission monochromators (2.1 nm/mm of dispersion; 1200 grooves/mm) and a TBX-04 single photon-counting detector. The powdered compounds were pressed to the wall of a quartz tube, and the measurements were performed using the right-angle mode. An excitation wavelength of 420 nm, a commonly used point although only part of a broad manifold, was used in all cases and the emission was monitored between 450 and 600 nm. The quantum yield measurements were performed by using an absolute photoluminescence quantum yield spectrometer Hamamatsu Quantaurus C11347 and exciting the samples between 300 and 400 nm.

References

- [1] See, for example: a) H. D. Burrows, M. da G. Miguel, *Adv. Colloid Inter. Sci.* **2001**, 89–90, 485–496; b) A. Brachmann, G. Geipel, G. Bernhard, H. Nitsche, *Radiochim. Acta* **2002**, 90, 147–153; c) M. P. Redmond, S. M. Cornet, S. D. Woodall, D. Whittaker, D. Collison, M. Helliwell, L. S. Natrajan, *Dalton Trans.* **2011**, 40, 3914–3926; d) G. Liu, N. P. Deifel, C. L. Cahill, V. V. Zhurov, A. A. Pinkerton, *J. Phys. Chem. A* **2012**, 116, 855–864; e) L. S. Natrajan, *Coord. Chem. Rev.* **2012**, 256, 1583–1603; f) R. G. Surbella, III, M. A. Andrews, C. L. Cahill, *J. Solid State Chem.* **2016**, 236, 257–271; g) S. Chorazy, J. J. Zakrzewski, M. Reczyński, B. Sieklucka, *Chem. Commun.* **2019**, 55, 3057–3060; h) M.

- Demnitz, S. Hilpmann, H. Lösch, F. Bok, R. Steudtner, M. Patzschke, T. Stumpf, N. Huittinen, *Dalton Trans.* **2020**, 49, 7109–7122.
- [2] a) K. X. Wang, J. S. Chen, *Acc. Chem. Res.* **2011**, 44, 531–540; b) M. B. Andrews, C. L. Cahill, *Chem. Rev.* **2013**, 113, 1121–1136; c) T. Loiseau, I. Mihalcea, N. Henry, C. Volkringer, *Coord. Chem. Rev.* **2014**, 266–267, 69–109; d) J. Su, J. S. Chen, *Struct. Bond.* **2015**, 163, 265–296.
- [3] a) S. Hickam, P. C. Burns, *Struct. Bonding (Berlin, Ger.)* **2017**, 173, 121–154; b) P. Thuéry, J. Harrowfield, *Dalton Trans.* **2017**, 46, 13660–13667.
- [4] a) J. Heine, K. Müller-Buschbaum, *Chem. Soc. Rev.* **2013**, 42, 9232–9242; b) J. Q. Liu, Z. D. Luo, Y. Pan, A. Kumar Singh, M. Trivedi, A. Kumar, *Coord. Chem. Rev.* **2020**, 406, 213145.
- [5] a) J. Xie, Y. Wang, W. Liu, X. Yin, L. Chen, Y. Zou, J. Diwu, Z. Chai, T. E. Albrecht-Schmitt, G. Liu, S. Wang, *Angew. Chem. Int. Ed.* **2017**, 56, 7500–7504; b) Y. Wang, X. Yin, W. Liu, J. Xie, J. Chen, M. A. Silver, D. Sheng, L. Chen, J. Diwu, N. Liu, Z. Chai, T. E. Albrecht-Schmitt, S. Wang, *Angew. Chem. Int. Ed.* **2018**, 57, 7883–7887.
- [6] Y. Zhang, L. Chen, Z. Liu, W. Liu, M. Yuan, J. Shu, N. Wang, L. He, J. Zhang, J. Xie, X. Chen, J. Diwu, *ACS Appl. Mater. Interfaces* **2020**, 12, 16648–16654.
- [7] X. Wang, Y. Wang, X. Dai, M. A. Silver, W. Liu, Y. Li, Z. Bai, D. Gui, L. Chen, J. Diwu, R. Zhou, Z. Chai, S. Wang, *Chem. Commun.* **2018**, 54, 627–630.
- [8] a) K. E. Knope, D. T. de Lill, C. E. Rowland, P. M. Cantos, A. de Bettencourt-Dias, C. L. Cahill, *Inorg. Chem.* **2012**, 51, 201–206; b) J. Xie, Y. Wang, M. A. Silver, W. Liu, T. Duan, X. Yin, L. Chen, J. Diwu, Z. Chai, S. Wang, *Inorg. Chem.* **2018**, 57, 575–582; c) J. A. Ridenour, C. L. Cahill, *CrystEngComm* **2018**, 20, 4997–5011.

- [9] a) X. Deng, Z. Li, H. Garcia, *Chem. Eur. J.* **2017**, *28*, 11189–11209; b) Q. Wang, Q. Gao, A. M. El-Anizi, A. Nafady, S. Ma, *Inorg. Chem. Front.* **2020**, *7*, 300–339.
- [10] J. Harrowfield, P. Thuéry, *Chemistry* **2020**, *2*, 63–79.
- [11] a) Z. T. Yu, Z. L. Liao, Y. S. Jiang, G. H. Li, J. S. Chen, *Chem. Eur. J.* **2005**, *11*, 2642–2650; b) J. A. Nieweg, K. Lemma, B. G. Trewyn, V. S.-Y. Lin, A. Bakac, *Inorg. Chem.* **2005**, *44*, 5641–5648; c) Z. L. Liao, G. D. Li, M. H. Bi, J. S. Chen, *Inorg. Chem.* **2008**, *47*, 4844–4853; d) V. Krishna, V. S. Kamble, N. M. Gupta, P. Selvam, *J. Phys. Chem. C* **2008**, *112*, 15832–15843; e) P. A. Kolinko, T. N. Fillipov, D. V. Kozlov, V. N. Parmon, *J. Photochem. Photobiol. A: Chemistry* **2012**, *250*, 72–77; f) Y. N. Hou, X. T. Xu, N. Xing, F. Y. Bai, S. B. Duan, Q. Sun, S. Y. Wei, Z. Shi, H. Z. Zhang, Y. H. Xing, *ChemPlusChem* **2014**, *79*, 1304–1315; g) W. Yang, W. G. Tiang, X. X. Liu, L. Wang, Z. M. Sun, *Cryst. Growth Des.* **2014**, *14*, 5904–5911; h) H. H. Li, X. H. Zeng, H. Y. Wu, X. Jie, S. T. Zheng, Z. R. Chen, *Cryst. Growth Des.* **2015**, *15*, 10–13; i) F. M. Khandan, D. Afzali, G. Sargazi, M. Gordan, *J. Mater. Sci.: Mater. Electron.* **2018**, *29*, 18600–18613.
- [12] P. Thuéry, Y. Atoini, J. Harrowfield, *Inorg. Chem.* **2019**, *58*, 870–880.
- [13] P. Thuéry, Y. Atoini, J. Harrowfield, *Cryst. Growth Des.*, in the press, DOI: .
- [14] W. Liu, E. Song, L. Cheng, L. Song, J. Xie, G. Li, Y. Zhang, Y. Wang, Y. Wang, Z. Xia, Z. Chai, S. Wang, *Chem. Mater.* **2019**, *31*, 9684–9690.
- [15] J. M. Harrowfield, N. Lugan, G. H. Shahverdizadeh, A. A. Soudi, P. Thuéry, *Eur. J. Inorg. Chem.* **2006**, 389–396.
- [16] a) C. R. Groom, I. J. Bruno, M. P. Lightfoot, S. C. Ward, *Acta Crystallogr., Sect. B* **2016**, *72*, 171–179; b) R. Taylor, P. A. Wood, *Chem. Rev.* **2019**, *119*, 9427–9477.
- [17] A. Immirzi, G. Bombieri, S. Degetto, G. Marangoni, *Acta Crystallogr., Sect. B* **1975**, *31*, 1023–1028.

- [18] a) P. M. Cantos, M. Frisch, C. L. Cahill, *Inorg. Chem. Commun.* **2010**, *13*, 1036–1039; b) R. C. Severance, A. J. Cortese, M. D. Smith, H. C. zur Loye, *J. Chem. Cryst.* **2013**, *43*, 171–177; c) Z. X. Si, W. Xu, Y. Q. Zheng, *J. Solid State Chem.* **2016**, *239*, 139–144.
- [19] B. Masci, P. Thuéry, *CrystEngComm* **2008**, *10*, 1082–1087.
- [20] a) N. W. Alcock, T. J. Kemp, S. M. Roe, J. Leciejewicz, *Inorg. Chim. Acta* **1996**, *248*, 241–246; b) R. C. Severance, S. A. Vaughn, M. D. Smith, H. C. zur Loye, *Solid State Sci.* **2011**, *13*, 1344–1353; c) M. B. Andrews, C. L. Cahill, *CrystEngComm* **2011**, *13*, 7068–7078; d) L. Lv, B. Chen, J. Liu, J. Chen, C. Xu, Y. Yang, *Dalton Trans.* **2019**, *48*, 566–577;
- [21] a) B. Masci, P. Thuéry, *Cryst. Growth Des.* **2008**, *8*, 1689–1696; b) P. Thuéry, B. Masci, *Cryst. Growth Des.* **2010**, *10*, 716–725.
- [22] S. Li, L. X. Sun, J. C. Ni, Z. Shi, Y. H. Xing, D. Shang, F. Y. Bai, *New J. Chem.* **2017**, *41*, 3073–3081.
- [23] See, for example: a) G. Marangoni, S. Degetto, R. Graziani, G. Bombieri, E. Forsellini, *J. Inorg. Nucl. Chem.* **1974**, *36*, 1787–1794; b) M. Frisch, C. L. Cahill, *Dalton Trans.* **2006**, 4679–4690; c) M. Mirzaei, H. Eshtiagh-Hosseini, V. Lippolis, H. Aghabozorg, D. Kordestani, A. Shokrollahi, R. Aghaei, A. J. Blake, *Inorg. Chim. Acta* **2011**, *370*, 141–149; d) A. B. Yusov, V. I. Mishkevich, A. M. Fedoseev, M. S. Grigor'ev, *Radiochemistry* **2013**, *55*, 269–278; e) C. Xu, G. Tian, S. J. Teat, L. Rao, *Inorg. Chem.* **2013**, *52*, 2750–2756; f) P. Thuéry, *CrystEngComm* **2013**, *15*, 6533–6545; g) A. S. Jayasinghe, M. K. Payne, T. Z. Forbes, *J. Solid State Chem.* **2017**, *254*, 25–31.
- [24] a) M. C. Etter, J. C. MacDonald, J. Bernstein, *Acta Crystallogr., Sect. B* **1990**, *46*, 256–262; b) J. Bernstein, R. E. Davis, L. Shimoni, N. L. Chang, *Angew. Chem. Int. Ed.* **1995**, *34*, 1555–1573.
- [25] A. L. Spek, *Acta Crystallogr., Sect. D* **2009**, *65*, 148–155.

- [26] M. A. Spackman, D. Jayatilaka, *CrystEngComm* **2009**, *11*, 19–32.
- [27] S. K. Wolff, D. J. Grimwood, J. J. McKinnon, M. J. Turner, D. Jayatilaka, M. A. Spackman, *CrystalExplorer*; University of Western Australia: Crawley, Australia, 2012.
- [28] a) R. Taylor, O. Kennard, *J. Am. Chem. Soc.* **1982**, *104*, 5063–5070; b) G. R. Desiraju, *Acc. Chem. Res.* **1996**, *29*, 441–449.
- [29] B. Masci, P. Thuéry, *Polyhedron* **2005**, *24*, 229–237.
- [30] D. Hall, A. D. Rae, T. N. Waters, *Acta Crystallogr.* **1965**, *19*, 389–395.
- [31] I. Dance, M. Scudder, *Chem. Eur. J.* **1996**, *2*, 481–486.
- [32] a) B. F. Mentzen, J. P. Puaux, H. Loiseleur, *Acta Crystallogr., Sect. B* **1977**, *33*, 1848–1851; b) S. D. le Roux, A. Van Tets, H. W. W. Adrian, *Acta Crystallogr., Sect. B* **1979**, *35*, 3056–3057; c) P. Thuéry, *CrystEngComm* **2013**, *15*, 6533–6545; d) Q. Zhu, R. Shang, S. Chen, C. Liu, Z. Wang, S. Gao, *Inorg. Chem.* **2014**, *53*, 8708–8716.
- [33] a) P. Thuéry, J. Harrowfield, *Cryst. Growth Des.* **2016**, *16*, 7083–7093; b) P. Thuéry, Y. Atoini, J. Harrowfield, *Inorg. Chem.* **2019**, *58*, 567–580; c) P. Thuéry, Y. Atoini, J. Harrowfield, *Cryst. Growth Des.* **2019**, *19*, 4109–4120.
- [34] C. A. Stackhouse, S. Ma, *Polyhedron* **2018**, *145*, 154–165.
- [35] P. Thuéry, J. Harrowfield, *Inorg. Chem.* **2017**, *56*, 13464–13481.
- [36] G. K. Liu, M. P. Jensen, *Chem. Phys. Lett.* **2010**, *499*, 178–181.
- [37] a) H. D. Burrows, S. J. Formosinho, M. da G. Miguel, F. Pinto Coelho, *J. Chem. Soc., Faraday Trans. 1* **1976**, *72*, 163–171; b) A. T. Kerr, C. L. Cahill, *Cryst. Growth Des.* **2014**, *14*, 1914–1921; c) A. T. Kerr, C. L. Cahill, *Cryst. Growth Des.* **2014**, *14*, 4094–4103; d) J. A. Ridenour, M. M. Pyrch, Z. J. Manning, J. A. Bertke, C. L. Cahill, *Acta Crystallogr., Sect. C* **2017**, *73*, 588–592; e) A. T. Kerr, J. A. Ridenour, A. A. Noring, C. L.

- Cahill, *Inorg. Chim. Acta* **2019**, 494, 204–210; f) G. E. Gomez, J. A. Ridenour, N. M. Byrne, A. P. Shevchenko, C. L. Cahill, *Inorg. Chem.* **2019**, 58, 7243–7254.
- [38] P. M. Almond, C. E. Talley, A. C. Bean, S. M. Peper, T. E. Albrecht-Schmitt, *J. Solid State Chem.* **2000**, 154, 635–641.
- [39] G. Zucchi, O. Maury, P. Thuéry, F. Gumy, J. C. G. Bünzli, M. Ephritikhine, *Chem. Eur. J.* **2009**, 15, 9686–9696.
- [40] See, for example: P. Thuéry, J. Harrowfield, *CrystEngComm.* **2016**, 18, 3905–3918.
- [41] H. D. Burrows, T. J. Kemp, *Chem. Soc. Rev.* **1974**, 3, 139–165.
- [42] S. Maji, S. Kumar, K. Sankaran, *Radiochim. Acta* **2017**, 108, 604–608.
- [43] See, for example: P. Thuéry, Y. Atoini, J. Harrowfield, *Dalton Trans* **2020**, 49, 817–828.
- [44] P. Thuéry, Y. Atoini, J. Harrowfield, *Inorg. Chem.* **2020**, 59, 2923–2936.
- [45] Y. Zhang, L. Chen, J. Guan, X. Wang, S. Wang, J. A. Diwu, *Dalton Trans.* **2020**, 49, 3676–3679.
- [46] P. Thuéry, J. Harrowfield, *Cryst. Growth Des.* **2018**, 18, 5512–5520.
- [47] R. W. W. Hooft, *COLLECT*, Nonius BV: Delft, The Netherlands, 1998.
- [48] Bruker AXS (2019). *APEX3*. Version 2019.1-0. Madison, Wisconsin, USA.
- [49] Z. Otwinowski, W. Minor, *Methods Enzymol.* **1997**, 276, 307–326.
- [50] Bruker Nano, Inc. (2019). *SAINT*. Version 8.40A. Madison, Wisconsin, USA.
- [51] a) Bruker AXS (2016). *SADABS*. Version 2016/2. Madison, Wisconsin, USA; b) L. Krause, R. Herbst-Irmer, G. M. Sheldrick, D. Stalke, *J. Appl. Crystallogr.* **2015**, 48, 3–10.
- [52] G. M. Sheldrick, *Acta Crystallogr., Sect. A* **2015**, 71, 3–8.
- [53] G. M. Sheldrick, *Acta Crystallogr., Sect. C* **2015**, 71, 3–8.
- [54] C. B. Hübschle, G. M. Sheldrick, B. Dittrich, *J. Appl. Crystallogr.* **2011**, 44, 1281–1284.

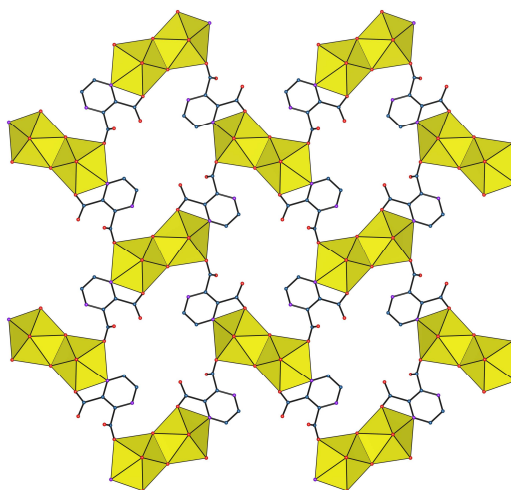
- [55] L. J. Farrugia, *J. Appl. Crystallogr.* **2012**, *45*, 849–854.
- [56] K. Momma, F. Izumi, *J. Appl. Crystallogr.* **2011**, *44*, 1272–1276.
- [57] V. A. Blatov, A. P. Shevchenko, D. M. Proserpio, *Cryst. Growth Des.* **2014**, *14*, 3576–3586.

Table of Contents Entry

Optimizing Photoluminescence Quantum Yields in Uranyl Dicarboxylate Complexes: Further Investigations of 2,5-, 2,6- and 3,5-Pyridinedicarboxylates and 2,3-Pyrazinedicarboxylate

Pierre Thuéry, Youssef Atoini, Sotaro Kusumoto, Shinya Hayami, Yang Kim, Jack Harrowfield

Key Topic: Photoluminescent uranyl complexes



Zero-, mono- and dipericodic homo- or heterometallic uranyl ion complexes were obtained with 2,5-, 2,6- and 3,5-pyridinedicarboxylates and 2,3-pyrazinedicarboxylate ligands. All are luminescent and one of them has the highest photoluminescence quantum yield reported for a uranyl ion carboxylate complex.